

# Modeling the deposition of fluorescent whitening agents on cotton fabrics

Bueno, Laura; Amador, Carlos; Bakalis, Serafim

DOI:  
[10.1002/aic.16001](https://doi.org/10.1002/aic.16001)

License:  
Creative Commons: Attribution (CC BY)

*Document Version*  
Publisher's PDF, also known as Version of record

*Citation for published version (Harvard):*  
Bueno, L, Amador, C & Bakalis, S 2018, 'Modeling the deposition of fluorescent whitening agents on cotton fabrics', *AIChE Journal*, vol. 64, no. 4, pp. 1305-1316. <https://doi.org/10.1002/aic.16001>

[Link to publication on Research at Birmingham portal](#)

## General rights

Unless a licence is specified above, all rights (including copyright and moral rights) in this document are retained by the authors and/or the copyright holders. The express permission of the copyright holder must be obtained for any use of this material other than for purposes permitted by law.

- Users may freely distribute the URL that is used to identify this publication.
- Users may download and/or print one copy of the publication from the University of Birmingham research portal for the purpose of private study or non-commercial research.
- User may use extracts from the document in line with the concept of 'fair dealing' under the Copyright, Designs and Patents Act 1988 (?)
- Users may not further distribute the material nor use it for the purposes of commercial gain.

Where a licence is displayed above, please note the terms and conditions of the licence govern your use of this document.

When citing, please reference the published version.

## Take down policy

While the University of Birmingham exercises care and attention in making items available there are rare occasions when an item has been uploaded in error or has been deemed to be commercially or otherwise sensitive.

If you believe that this is the case for this document, please contact [UBIRA@lists.bham.ac.uk](mailto:UBIRA@lists.bham.ac.uk) providing details and we will remove access to the work immediately and investigate.

# Modeling the Deposition of Fluorescent Whitening Agents on Cotton Fabrics

Laura Bueno 

School of Chemical Engineering, University of Birmingham, Birmingham B15 2TT, U.K.

Carlos Amador

Newcastle Innovation Centre, Procter & Gamble Ltd., Newcastle Upon Tyne NE12 9BZ, U.K.

Serafim Bakalis

Dept. of Chemical and Environmental Engineering, University of Nottingham, Nottingham NG7 2RD, U.K.

DOI 10.1002/aic.16001

Published online October 27, 2017 in Wiley Online Library (wileyonlinelibrary.com)

*The adsorption of two widely used fluorescent whitening agents (FWAs) on unbrightened cotton fabrics has been investigated as a function of temperature, hardness of the wash liquor, initial concentration of FWA in solution, and fabric to wash liquor ratio. Sorption efficiencies of FWAs have been studied using a UV spectrophotometry technique. A mechanistic model has been developed to describe the dissolution process of FWAs, convective mass transport into the fabrics, diffusion in the stagnant layer to the fabrics' surface, and adsorption of FWAs on cotton fabrics. Dual porosity of the fabrics (inter-yarn and intra-yarn porosity) has been considered by allowing two different regions (outer and inner areas of the cotton fabrics) where FWAs molecules can diffuse and adsorb. Good agreement between experimental and predicted whiteness benefit by the proposed mathematical model has been observed for the range of variables considered. © The Authors AICHE Journal published by Wiley Periodicals, Inc. on behalf of 2017 American Institute of Chemical Engineers AICHE J, 64: 1305–1316, 2018*

**Keywords:** FWAs, optical brighteners, whitening, adsorption

## Introduction

Many organic fabrics such as cotton absorb in the short UV-region extending into the blue region of the spectrum which promotes a yellowing shade on the textiles. The extent of this shade depends on some properties of the polymer such as the number of conjugated systems, the degree of substitution, as well as the degradation products.<sup>1</sup> Bleaching of cotton textiles is carried out during its processing prior to dyeing and further finishing steps to remove the yellowish color and achieve a white appearance. The most common bleaching agent used industrially is hydrogen peroxide.<sup>2,3</sup> However, gradual yellowing and whiteness loss of used textile items occur over time due to several causes like accumulation and aging of unrecovered oily soils such as human sebum or particulate soils.<sup>4–7</sup> Thus, during the washing process of textiles in a commercial washing machine, different whiteness maintenance transformations take place, namely (a) soil removal from fabrics' structure, (b) suspension and antiredeposition of removed soil, (c) bleaching of soils remaining in fabrics, (d) deposition of shading dye actives, which are used to shift the yellowness of fabrics to a more preferred blue hue, and (e) deposition of

fluorescent whitening agents (FWAs) which are also known as optical brighteners.

FWAs are widely used in the textile and paper industry for improvement and maintenance of whiteness. These molecules absorb light in the UV region (340–360 nm) and emit on the blue region of the visible spectrum (440–460 nm). Thus, not only the yellowish of the fabrics is compensated but also more visible light is emitted resulting in a whiter and brighter appearance of the textiles.<sup>8,9</sup>

The majority of the FWAs used in the detergent industry present affinity for cotton fabrics. The most important FWAs used for this substrate contain two sulphonate groups and can be divided into two main categories depending on the type of chemical group present on their structure: distyrylbiphenyl (DSBP) or diaminostilbene (DAS).<sup>10</sup> These groups are the chromophores of the FWAs where the electron transitions induced by the absorption of light in the UV region of the spectrum takes place. The optical properties of the chromophores can be modified by substituents that may promote an intensification of the fluorescence depending on their location on the chromophore.<sup>9</sup>

The change in appearance of textiles due to the adsorption of FWAs can be assessed by reflectance spectroscopy which is one of the main techniques used for color assessment.<sup>11</sup> The most common system for color measurement is the CIE system (Commission Internationale de l'Eclairage).

Desirable attributes of the FWAs molecules are (i) high solubility of the molecules and kinetics of dissolution, (ii) high partition coefficient toward the fabric surface to improve

Additional Supporting Information may be found in the online version of this article.

Correspondence concerning this article should be addressed to L. Bueno at lxb269@bham.ac.uk.

© The Authors AICHE Journal published by Wiley Periodicals, Inc. on behalf of 2017 American Institute of Chemical Engineers

**Table 1. Characterization of Cotton Textiles**

Property	Flat cotton	Terry Cotton	Knitted cotton	Polycotton	Method
Initial $b^*$ value ( $L^*a^*b^*$ colorspace)	−0.5	−14.8	−14	−8	Spectrophotometry
Specific surface area (m <sup>2</sup> /kg)	12.38	3.93	6.60	17.13	Gravimetric technique
Yarn diameter (m)	$218 \times 10^{-6}$ $\pm 20 \times 10^{-6}$	$868 \times 10^{-6}$ $\pm 20 \times 10^{-6}$	$288 \times 10^{-6}$ $\pm 20 \times 10^{-6}$	$189 \times 10^{-6}$ $\pm 20 \times 10^{-6}$	SEM
Fiber diameter (m)	$16 \times 10^{-6}$ $\pm 3 \times 10^{-6}$	$13 \times 10^{-6}$ $\pm 3 \times 10^{-6}$	$16 \times 10^{-6}$ $\pm 3 \times 10^{-6}$	$12 \times 10^{-6}$ $\pm 3 \times 10^{-6}$	SEM

deposition level efficiency, and (iii) high stability to sunlight is also essential as the oxidative degradation of the molecules leads to the formation of products that cause yellowing of fabrics. The photochemical reactions involve a reversible photoisomerization of the FWAs followed by an irreversible photodegradation process that leads to the yellowing of the fabrics.<sup>12–14</sup> It has been reported that FWAs present different lightfastness (resistance to fading when exposed to sunlight) so that DSBP type presents a superior lightfastness than that of DAS-type FWAs, promoting a lower decrease on the whiteness of the textiles when they are exposed to light.<sup>15</sup>

Cotton textiles can be described as a nonhomogeneous porous media formed by two main porosities, a comparatively large porosity due to the spaces in between the yarns and a second and smaller porosity due to the spaces in between the fibers forming the yarns.<sup>16</sup>

The transport of the FWAs molecules from the bulk solution to the textiles surface as well as the surface accessibility during the washing process determines the rate and magnitude of adsorption when the adsorption process in itself is not rate limiting.<sup>17</sup> Mass-transfer phenomena in textile porous media have been extensively studied in the past.<sup>18–20</sup> Van den Brekel<sup>21</sup> has concluded that there are two existing regimens for the flow inside a textile as a function of the textile porosity, existing a relatively fast flow between the yarns (inter-yarn porosity) and a much slower diffusive flow in the smaller spaces in between the fibers forming the yarns (intra-yarn porosity). Moholkar and Warmoeskerken<sup>22</sup> have developed a model to describe the flow through textiles based on the relative resistances present in each region.

Ganguli and Eendenburg<sup>23</sup> have studied the mass transfer through textiles in an agitated bath and have suggested that the diffusive region is dependent on the mechanical action of the system so that with increasing agitation, the thickness of this region is reduced due to greater degree of flow penetration from the bath into the textiles' structure. Warmoeskerken et al.<sup>24</sup> have also concluded that the role of the mechanical action experienced by the textiles in the washing machine during the washing process promotes the squeezing of textiles which leads to the reduction of the stagnant region.

The amount of FWAs deposited on the textiles can be determined using a UV spectroscopy technique. Yoon and Chai<sup>25,26</sup> have tracked the adsorption of two commercial additives on the fiber surface of papermaking fibrous solutions. XianNan et al.<sup>27</sup> have studied the adsorption behavior of a FWA on a paper fibrous suspension using this technique. Iamazaki and Atvars<sup>8,28</sup> have studied the impact of surfactants and salts on the sorption of FWAs onto fibers, concluding that surfactant charge and concentration influences the sorption of FWAs. Oppositely charged surfactants respect to FWAs have a positive effect on the sorption process due to the electrostatic interactions. Salts induce changes on the critical micelle

concentration of the surfactants promoting a beneficial effect on the FWAs sorption.

However, to the best of our knowledge, there is no study that deals with the modeling of all the transformations involved in the adsorption of FWAs during the washing process. Therefore, the aim of the present work is to quantitatively assess and model the adsorption behavior of two FWAs typically used in detergent formulations onto flat cotton fabrics as a function of temperature, water hardness, initial concentration of FWAs in solution, fabric to wash liquor ratio, and concentration of detergent formulation in the system.

### Materials

Water hardness is controlled by the amount of calcium and magnesium ions salts dissolved in the water<sup>29</sup> by adding  $\text{CaCl}_2 \cdot 2\text{H}_2\text{O}$  and  $\text{MgCl}_2 \cdot 6\text{H}_2\text{O}$  (VWR chemicals), 4,4'-DSBP sulfonic acid sodium salt (Tinopal CBS, Sigma Aldrich), and 4,4'-DAS-2,2'-disulfonic acid sodium salt (Tinopal DMS, Sigma Aldrich). Unbrightened and bleached flat cotton fabrics are used as model textiles (Warwick Equest, UK), knitted cotton, polycotton, and terry towel textiles (WFK, Germany) are used to test the impact of fabric structure on FWAs' performance, and cellulose powder (20  $\mu\text{m}$ , Sigma Aldrich) is used for the characterization of cellulose zeta potential of the system. A powder detergent (Procter and Gamble) with nil whitening actives content is used as base formulation for all experiments. The detergent is composed by 5%–15% anionic surfactants, <5% nonionic surfactants, <5% zeolites, phosphonates, and polycarboxylates, <5% enzymes, and <5% perfumes.

### Characterization of cotton textiles

Main characteristics of unbrightened and bleached cotton textiles are summarized on Table 1. Figure 1 represents a SEM image of dried flat cotton fabric and terry cotton, respectively. It can be observed how the terry cotton fabric presents a thicker yarn (higher number of fibers forming the yarn) compared to flat cotton; however, the fiber diameter remains the same in both cases.

### Apparatus

The schematic diagram of the experimental setup is represented in Figure 2. A UV–Cary 60S spectrophotometer online probe (Agilent Technologies) is used to monitor the absorbance of the FWAs in solution in real time. The UV probe is protected with a metal frame to avoid the deposition of small fibers on the probe which then alter the absorbance signal increasing the experimental noise.

To be able to track the concentration of FWAs present in solution by spectrophotometry, a calibration curve that correlates the concentration in solution with the resulting absorbance is required. For that purpose, the spectrum (200–

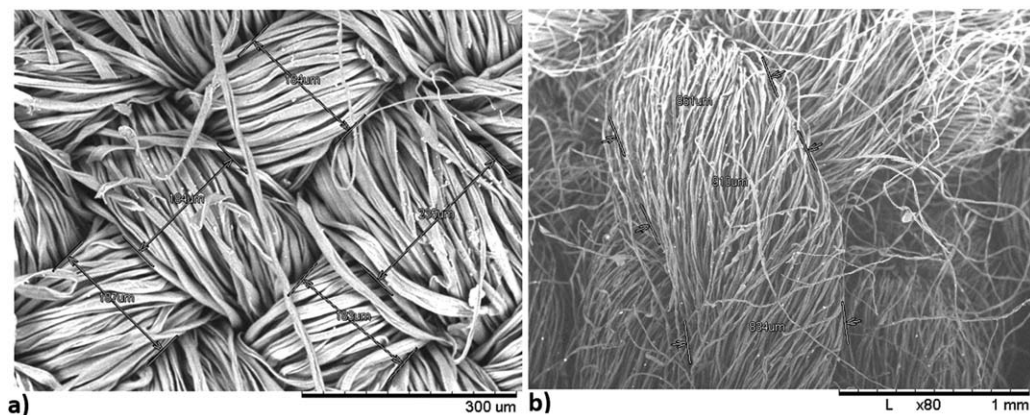


Figure 1. SEM image of (a) dried flat cotton fabric and (b) dried terry cotton fabric.

700 nm) of both FWAs has been obtained and the wavelength of maximum absorbance selected ( $\lambda_{\text{max}} = 350 \text{ nm}$ ). This technique allows obtaining high time-resolution data of full deposition kinetics (dissolution/active transport and deposition) on a single experiment. The calibration curve of each FWA was obtained by preparing solutions of different concentration and measuring the absorbance at  $\lambda = 350 \text{ nm}$ . Different calibration curves were obtained for several temperatures, water hardness and detergent formulation concentration to study the potential effect of each variable on the absorbance value. Absorbance measurements of each solution were carried out filtering and nonfiltering the samples with a syringe filter of  $0.45 \mu\text{m}$  pore size (Fisher Scientific) to account for possible differences probably due to the formation of crystals from both the detergent, hardness and FWAs or due to the presence of undissolved FWA (solubility dependence on temperature).

### Experimental procedure

The main set of experiments were carried out with predissolved FWA to study the FWA transport independently. Later on, dissolution and transport were combined within the model and experimentally validated. As shown in Figure 2, 0.8 L of solvent (deionized water) was introduced in a tergotometer, which consists of a cylindrical vessel continuously stirred by a two blade flat impeller. Initially, salts used to control hardness of the wash liquor were added to the tergotometer and stirred for 10 min to ensure complete dissolution. Afterward, detergent formulation with nil FWA content was added to the solution and stirred for 30 min. Finally, FWAs were added to the vessel containing the dissolved salts and detergent and stirred for 30 min more. Stirring is maintained constant in all cases at a speed of 200 rpm. At this moment, unbrightened cotton fabrics ( $5 \text{ cm} \times 5 \text{ cm}$ ) were added to the tergotometer and the stirring speed decreased to 100 rpm to avoid too much abrasion between the fabrics leading to a very high release of fibers which would then promote an increase in the signal noise. As soon as the fabrics are added, the porosity is filled by the wash liquor due to capillary action bringing in FWAs into the fabrics' structure ( $\sim 3.7\%$  of the total mass of FWAs). Absorbance was monitored in real time at the peak wavelength of the FWAs ( $\lambda = 350 \text{ nm}$ ). After the experiment, the cotton fabrics were removed from the tergotometer and introduced in a 0.05-L syringe where they were compressed to remove the excess of wash liquor from the fabrics structure by applying a uniform force across all the fabrics. The degree of

compression was calculated based on the fabrics absorbency to achieve a similar degree of water removal to the one experienced by the textiles in a commercial front loader washing machine at the end of the wash cycle ( $\sim 1 \text{ kg water/1 kg fabric}$ ). Afterward, the fabrics were dried overnight at room temperature and the final color of the cotton fabrics was measured by reflectance spectrophotometry.

### Multicycle

Multicycle performance of FWAs depositing on flat woven cotton fabrics was studied following the methodology previously described for the washing process. Afterward, the cotton fabrics were rinsed for 5 min by introducing them in the same tergotometer system, containing 0.8-L deionized water at 293 K and 100 rpm. Then, the fabrics were removed from the tergotometer, and the excess of water eliminated from the fabrics structure as previously described using a syringe. Next, the fabrics were dried overnight at room temperature prior to conduct the color measurement by spectrophotometry. The fabrics were then submerged in deionized water to completely wet the textiles. Drying of textiles in outdoor conditions was replicated by introducing the fabrics in a solar simulating room, which is a dark room equipped with lamps with a light irradiance level that simulates solar conditions. Fabrics are hung on drying racks and exposed to the light from the lamps for 1 h to replicate the amount of sunlight received on an average 10 h exposure day in a hot country. Thus, this procedure

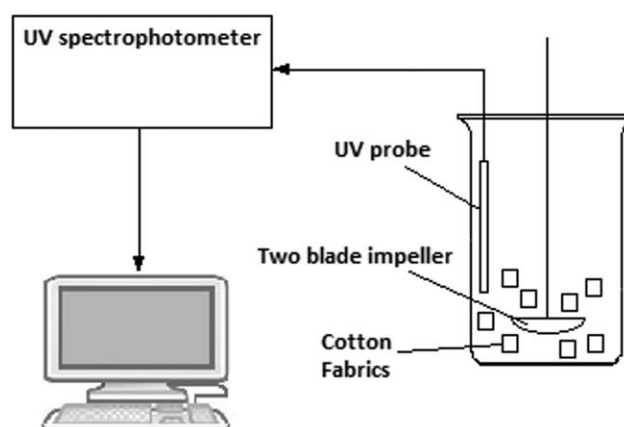


Figure 2. Schematic diagram of the experimental setup.



allows us to magnify the effect of sunlight on the yellowing of textiles. After 1 h, fabrics were removed from the solar simulating room and the color measured again to obtain the effect of sunlight degradation. This procedure constitutes one complete wash cycle of the textiles.

### Design of experiments

The following variables and ranges were considered for the study of FWAs adsorbing on cotton fabrics: temperature (293–333 K), hardness (0–20 gpg), fabric to wash liquor ratio (0.0187–0.0375 kg/kg), detergent concentration (0–5000 ppm), and initial concentration of FWAs (2.6–35 ppm). The range selected for the fabric to wash liquor ratio is lower than the one typically found in real washing machine conditions (~0.07 to 0.2 kg/kg) to obtain more reproducible results by reducing the noise/signal ratio. During the washing process, fabrics release fibers which can then get trapped in the UV probe promoting a significant increase of the experimental noise; therefore by maintaining a low fabric to wash liquor ratio, the noise is minimized. In addition, fabric mixing within the tergotometer is better at low to moderate fabric to wash liquor ratios. However, the mechanistic model can then be used to extrapolate results to higher fabric to wash liquor ratios. The FWAs concentration range selected is slightly higher than the one typically used in detergent formulations to magnify the absorbance signal at  $\lambda_{\text{max}} = 350$  nm and improve the detection of FWAs adsorption on textiles using this technique.

Two different design of experiments were created for nil and 5000 ppm of Ariel detergent formulation in solution for each FWA. The design of experiments was conducted considering linear terms for all variables, interaction terms to second degree for all variables except for fabric to wash liquor ratio which was studied as a single variable effect, and quadratic terms for temperature and concentration. Although the dissolution and transport models are mechanistic, the dependence of the isotherm coefficient with these variables is statistically fitted.

Four additional multicycle experiments were carried out for both FWAs separately with an initial concentration in solution of 35.1 ppm for Tinopal DMS and 7.8 ppm for Tinopal CBS. Each cycle was conducted at the following fixed experimental conditions for the washing step: 293 K, 5000 ppm Ariel detergent formulation, 0 gpg spiked hardness, and 0.01875 kg/kg for the fabric to wash liquor ratio.

Blank experiments with nil FWAs concentration were also conducted to understand whether the presence of any of the different actives in the detergent formulation could alter the  $L^*a^*b^*$  values of the cotton fabrics.

## Methods

### Mobility measurements

To understand the effect of detergent concentration and hardness level on the cotton surface charge, the electrophoretic mobility of cellulose powder in aqueous solutions was measured at  $25.0 \pm 0.5^\circ\text{C}$  using a Zetasizer Nano ZS (Malvern Instruments) similarly to the method described by Iamazaki and Atvars.<sup>28</sup> Aqueous solutions with different electrolyte concentrations ( $\text{CaCl}_2 \cdot 2\text{H}_2\text{O}$  and  $\text{MgCl}_2 \cdot 6\text{H}_2\text{O}$  on a 3:1 molar ratio corresponding to 0–20 gpg hardness) were prepared with and without Ariel powder detergent formulation (5000 ppm). Afterward, cellulose powder was added to the solutions and

stirred at 200 rpm by a magnetic stirrer for 2 h prior to conduct the measurement. Blank experiments were conducted in all cases to remove the background signal and consider exclusively the signal due to the electrophoretic mobility of the cellulose (see Supporting Information Appendix 1). The average value of 10 consecutive measurements was considered for each sample. Zeta potential is calculated from the electrophoretic mobility data using Smoluchowski equation.<sup>30–32</sup>

### Color measurements

Color measurements of cotton textiles before and after wash were obtained by a reflectance spectrophotometer (Konica Minolta, CM-3610d) considering a  $10^\circ$  observer under CIE standard D65 illuminant (daylight, outdoor conditions).<sup>33,34</sup> Cotton fabrics' reflectance under D65 illuminant with the exclusion of UV component was similarly measured to obtain the reflectance of textiles without the action of FWAs, simulating indoor conditions which are relevant to understand the yellowing (change in shade) of fabrics due to sunlight degradation. CIE  $L^*a^*b^*$ <sup>35,36</sup> measurements were conducted in 10 fabrics per experiment, and three repeats per measurement were obtained.

### Scanning electron microscopy (SEM)

Surface characterization of cotton textiles was carried out using a Hitachi TM-1000 scanning electron microscope. Each fabric sample was fixed in a sample holder and examined with an appropriate acceleration voltage (15 kV) and suitable magnification.

## Modeling

Based on experimental data, the mechanism proposed for the deposition of FWAs on flat cotton fabrics is controlled by the following phenomena: (I) dissolution of FWAs in the bulk solution, (II) convective mass-transfer flow into the fabrics, (III) Fickian diffusion of FWA molecules to the fabric surface in the liquid stagnant layer within the yarns, (IV) adsorption/desorption on fabrics' surface (adsorption/desorption isotherms), and (V) resulting  $L^*a^*b^*$  values of fabrics for a given deposition concentration of FWA. Figure 3 represents a schematic diagram of the different phenomena considered in the system.

#### (I) Dissolution of FWAs

The Noyes–Whitney equation can be used to describe the particle dissolution rate when the process is controlled by the external mass transfer at the boundary of the particle

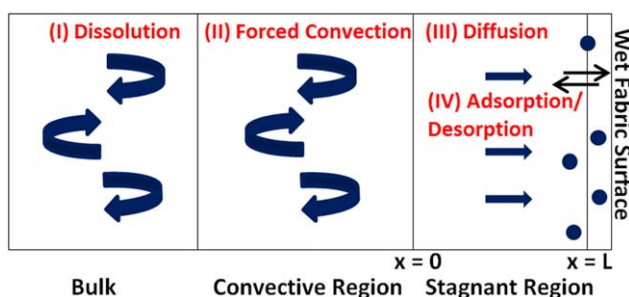


**Figure 3.** Schematic diagram of the regions considered in the system.

[Color figure can be viewed at [wileyonlinelibrary.com](http://wileyonlinelibrary.com)]

surface.<sup>37,38</sup> The dissolution rate can be expressed as follows for species  $i$

$$\frac{dM_i}{dt} = -K_i \cdot A_{i_l} \cdot (c_{\text{sat}_i} - c_{\text{solution}, i_l}) \quad (1)$$

where  $M_i$  (kg) is the undissolved mass at a given time,  $K_i$  (m/s) is the solid-liquid mass-transfer coefficient,  $A_{i_l}$  (m<sup>2</sup>) is the interfacial area,  $C_{\text{sat}_i}$  (kg/m<sup>3</sup>) is the saturation concentration of species  $i$ , and  $c_{\text{solution}, i_l}$  (kg/m<sup>3</sup>) is the concentration of species  $i$  in the bulk solution. Assuming that  $C_{\text{sat}_i} \gg c_{\text{solution}, i_l}$  and that the particles have spherical shape (which has been confirmed by SEM analysis of both FWAs particles), the undissolved mass and the interfacial area can be expressed as described by Cao et al.<sup>39</sup> Substituting in Eq. 1

$$\frac{dM_i}{dt} = -K_i \cdot A_{i_{l0}} \cdot C_{\text{sat}_i} \cdot \left(\frac{M_i}{M_{i0}}\right)^{2/3} \quad (2)$$

where  $M_{i0}$  (kg) and  $A_{i_{l0}}$  (m<sup>2</sup>) refers to initial undissolved mass and initial interfacial area of the particles, respectively.

## (II) Convective mass transfer flow into the fabrics

The mass balance for species  $i$  to the bulk is represented by Eq. 3

$$V_{\text{bulk}} \frac{dc_{\text{solution}, i, t}}{dt} = \frac{dM_i}{dt} + Q_F \cdot c_{\text{conv}, i, t} - Q_F \cdot c_{\text{solution}, i, t} \quad (3)$$

where  $V_{\text{bulk}}$  (m<sup>3</sup>) is the bulk volume,  $Q_F$  (m<sup>3</sup>/s) is the convective flow generated due to the hydrodynamics forces on the fabrics, and  $c_{\text{conv}, i, t}$  (kg/m<sup>3</sup>) is the concentration of species  $i$  in the convective region at time  $t$ . The mass balance to the convective region which is connected to the bulk via the convective flow is given by Eq. 4

$$V_{\text{conv.}} \cdot \frac{dc_{\text{conv}, i, t}}{dt} = -S_A \cdot D_i(T) \cdot \left. \frac{\partial c_i(x, t)}{\partial x} \right|_{x=0} - Q_F \cdot c_{\text{conv}, i, t} + Q_F \cdot c_{\text{solution}, i, t} \quad (4)$$

where  $D_i(T)$  (m<sup>2</sup>/s) is the diffusion coefficient of species at a given temperature  $T$  (K),  $L$  (m) is the thickness of the diffusive layer,  $c_i(x, t)$  is the concentration of species  $i$  at time  $t$  and position  $x$  of the diffusive layer domain, and  $S_A$  (m<sup>2</sup>) is the surface area of fabrics which can be expressed according to Eq. 5

$$S_A = S_{A_{\text{specific}}} \cdot M_F \quad (5)$$

where  $S_{A_{\text{specific}}}$  (m<sup>2</sup>/kg) is the specific apparent surface area and  $M_F$  (kg) is the fabric mass.

There is also an initial convective flow by capillarity when the dry fabrics are added into the wash liquor. This is not important in real-wash conditions where the detergent is added to the wash after the water has filled the fabrics' structure. The impact of this capillary flow in the present experiments is very low due to having a small fabric to water ratio (only ~3.7% of the total FWAs flows into the fabrics structure by capillary action potentially resulting in faster diffusion for this small fraction of the total FWAs deposited ~80%–90%).

## (III) Fickian Diffusion of molecules to the fabric surface

Due to the complex geometry of the fibers within the yarn (see Figure 1), a simplified system with a single Cartesian diffusion distance is first considered. According to Fick's first and second laws of diffusion, the change in concentration of species  $i$  in the diffusive layer over time can be expressed as described by Eq. 6

$$\frac{\partial c_i(x, t)}{\partial t} = D_i(T) \frac{\partial^2 c_i(x, t)}{\partial x^2} \quad (6)$$

The influence of temperature on the diffusion coefficient is given by Eq. 7 derived from the Stokes Einstein equation<sup>41</sup>

$$D_i(T) = D_i(T_{\text{ref}}) \cdot \frac{T/\mu}{T_{\text{ref}}/\mu_{\text{ref}}} \quad (7)$$

where  $D_i(T_{\text{ref}})$  (m<sup>2</sup>/s) is the diffusion coefficient of species  $i$  at the reference temperature ( $T_{\text{ref}} = 293$  K), and  $\mu$  (Pa s) and  $\mu_{\text{ref}}$  (Pa s) is the viscosity of the wash liquor at a given temperature and at the reference temperature, respectively. The viscosity of water as a function of temperature is well known and can be calculated according to the Arrhenius type of equation.<sup>42</sup>

## Boundary conditions

$$\text{For } x = 0 \quad c_i(x, t)|_{x=0} = c_{\text{solution}, i, t} \quad (8)$$

$$\text{For } x = L \quad D(T)_i \cdot \left. \frac{\partial c_i(x, t)}{\partial x} \right|_{x=L} = -\frac{d(c_{\text{adsorbed}, i, t})}{dt}$$

## Initial conditions

$$\text{Pre-wetted fabrics, } t = 0 \quad c_i(x, 0) = c_{\text{solution}, i, t=0} \quad (9)$$

$$\text{Non pre-wetted fabrics, } t = 0 \quad c_i(x, 0) = 0$$

The total volume of liquid ( $V_{\text{total}}$ , m<sup>3</sup>) is the sum of the volume of liquid present in the bulk region and the volume of liquid in the convective ( $V_{\text{conv}}$ , m<sup>3</sup>) and stagnant region ( $V_{\text{stagnant}}$ , m<sup>3</sup>) of the fabrics. It can be expressed as follows

$$V_{\text{total}} = V_{\text{Bulk}} + V_{\text{conv.}} + V_{\text{stagnant}} \quad (10)$$

$$V_{\text{stagnant}} = S_A \cdot L \quad (11)$$

It has been considered that the total surface area of the textiles available for the adsorption of FWAs is the apparent surface on both sides of the fabrics. This area is used as available area for adsorption instead of the individual fiber area to reduce the complexity of the model because, in the latter case, the layer for the diffusion of actives would be shared by multiple fibers, otherwise the volume of liquid present in the diffusive layer would be unrealistic. Furthermore it is believed that the apparent surface area of the fabrics may be the most important area to consider in the adsorption process as the availability of the fiber area would be reduced as we go deeper into the yarn due to the compression of fibers within the yarn, especially due to the fiber swelling during the washing process.

## (IV) Adsorption/Desorption on fabrics' surface

The kinetics of adsorption/desorption is considered instantaneous in comparison to the convective and diffusive processes.<sup>17</sup> Langmuir, Freundlich, and linear mathematical expressions<sup>43</sup> were considered for the fitting of equilibrium isotherms. A linear isotherm has been considered as it fits best the experimental data of both optical brighteners for the range of concentration considered (Eq. 12)

$$c_{\text{adsorbed}, i, t=t_{\text{eq}}} = c_{\text{eq}_i} \cdot c_i(x=L, t=t_{\text{eq}}) \quad (12)$$

where  $c_{\text{adsorbed}, i, t}$  (kg/m<sup>2</sup>) is the adsorbed concentration of species  $i$  in equilibrium,  $c_{\text{eq}_i}$  (m<sup>3</sup>/m<sup>2</sup>) is the partition coefficient, and  $c_i(x=L, t=t_{\text{eq}})$  (kg/m<sup>3</sup>) is the concentration in solution of species  $i$  in equilibrium with its adsorbed concentration.

## (V) Reflectance of fabrics

Measurement of the fabrics' reflectance by spectrophotometry allows us to correlate the change produced in the  $L^*a^*b^*$

values of the cotton fabrics before and after wash with the adsorbed concentration of FWAs, which is calculated by a mass balance as described below

$$c_{\text{solution},i,t=0} \cdot V_{\text{total}} = c_{\text{solution},i,t} \cdot V_{\text{total}} + c_{\text{adsorbed},i,t} \cdot S_{\text{specific}} \cdot M_F$$

$$c_{\text{adsorbed},i,t} = \frac{V_{\text{total}} (c_{\text{solution},i,t=0} - c_{\text{solution},i,t})}{S_{\text{specific}} \cdot M_F} \quad (13)$$

where the concentration of active in solution of species  $i$  at a given time is obtained from the absorbance measurements and the calibration curve that correlates the absorbance with the concentration of FWA in solution.

It is expected to observe a change mainly in the  $b^*$  color component ( $L^*a^*b^*$  colorspace) after the wash due to the FWAs' mechanism ( $db_{i,t}^*$ ), emitting light on the blue region of the visible spectrum, which has been experimentally confirmed. It has also been observed that the change produced on the other two color components due to the adsorption of FWAs is linearly correlated with the change in vector  $b^*$ . The relationship between  $db_{i,t}^*$  and the adsorbed concentration is given by Eq. 14, which is of the form of Michaelis-Menten equation<sup>44</sup>

$$db_{i,t}^* = \frac{P_{1i} \cdot P_{2i} \cdot c_{\text{adsorbed},i,t}}{1 + P_{2i} \cdot c_{\text{adsorbed},i,t}} \quad (14)$$

where  $P_{1i}$  and  $P_{2i}$  are fitting parameters of the species  $i$ . Reported values of  $db_{i,t}^*$  are normalized ( $db_{n,i,t}^*$ ) considering the maximum  $db_{i,t}^*$  experimentally obtained for the range of variables considered in the study.

To be able to predict the change in the  $b^*$  color component of the cotton textiles when both FWAs are present in solution, it is important to bear in mind that the relationship between the change in the  $b^*$  component ( $L^*a^*b^*$  colorspace) of the fabrics and the adsorbed concentration is not linear, and therefore, the combined action of both molecules cannot be obtained by linear addition of the  $db_{i,t}^*$  of each individual component.

A normalized adsorbed concentration ( $c_{\text{adsorbed},n,i,t}$ ) is defined as the adsorbed concentration of a given FWA divided by the maximum concentration obtained for the range of conditions considered in the study. The nonlinearity of the adsorbed concentration and  $db_{i,t}^*$  should be similar for both FWAs tested as a result of similar adsorption and quenching mechanisms. One would expect, the normalized curve of  $db_{i,t}^*$  to be similar in both cases as shown in Supporting Information Appendix 2. Using this, to obtain the resulting  $db_{\text{total},t}^*$  of textiles as a result of the combined action of both actives, a single curve of  $db_{i,t}^*$ -adsorbed concentration is required. In the present case, the curve corresponding to Tinopal CBS has been selected.

The adsorbed concentration of Tinopal CBS is calculated at a certain time based on dissolution kinetics, mass transfer, and adsorption isotherm. Next, to know the contribution from the second component on the total change in the  $b^*$  value of the cotton fabrics ( $db_{\text{total},t}^*$ ), an equivalent adsorbed concentration of Tinopal CBS due to the action of Tinopal DMS is required. For that purpose, the adsorbed concentration of Tinopal DMS is calculated as well as the corresponding  $db_{\text{DMS},t}^*$  using Eq. 14 as it was the only component in the system. Then, the equivalent adsorbed concentration of Tinopal CBS due to the impact of Tinopal DMS ( $c_{\text{equiv. ads, CBS}}$ , kg/m<sup>2</sup>) is calculated by Eq. 15

$$c_{\text{equiv. ads, CBS}} = \frac{db_{\text{DMS},t}^*}{P_{2 \text{ CBS}} \cdot (P_{1 \text{ CBS}} - db_{\text{DMS},t}^*)} \quad (15)$$

where the subscript DMS or CBS refers to Tinopal DMS or Tinopal CBS, respectively. The total change in the  $b^*$  component of the textiles ( $db_{\text{total},t}^*$ ) due to the presence of both FWAs molecules is therefore due to the adsorbed concentration of Tinopal CBS plus the equivalent adsorbed concentration due to the presence of Tinopal DMS.  $db_{\text{total},t}^*$  is then calculated using Eq. 16

$$db_{\text{total},t}^* = \frac{P_{1 \text{ CBS}} \cdot P_{2 \text{ CBS}} \cdot (c_{\text{adsorbed,CBS},t} + c_{\text{equiv. ads, CBS}})}{1 + P_{2 \text{ CBS}} \cdot (c_{\text{adsorbed,CBS},t} + c_{\text{equiv. ads, CBS}})} \quad (16)$$

This procedure has been experimentally validated as described in Supporting Information Appendix 2.

## Results and Discussion

### Dissolution of FWAs

Kinetics of dissolution of Tinopal DMS is greatly influenced by temperature whereas Tinopal CBS is very fast dissolving in any case. This will highly impact the adsorption performance of Tinopal DMS mainly for cold and short contact times due to less dissolved mass available in solution. It can be observed in Figure 4 that there is a portion of Tinopal DMS dissolving very fast regardless of the temperature and hardness conditions which may be due to the presence of a very broad particle-size distribution (PSD) of the raw material. Therefore, different size cuts have been considered for the modeling of the dissolution process. Unknown dissolution parameters are the kinetic constant, the initial interfacial area of particles and the concentration of saturation of species  $i$  which are captured by a kinetic constant, ( $k_i'$ , kg/s) as described by Eq. 17

$$k_i' = K_i \cdot A_{\text{Iio}} \cdot C_{\text{sat},i} \quad (17)$$

The kinetic dissolution constant depends on the temperature of the solvent, and in the case of Tinopal DMS it is also a function of the hardness present in the system. It can be expressed by Eq. 18 which has been experimentally obtained

$$k_{\text{DMS}}' = k_{\text{DMS},0\text{gpg}} \cdot [1 + 0.35 \cdot (T - 273)] \cdot (1 - H) + k_{\text{DMS},20\text{gpg}} \cdot [1 + 0.35 \cdot (T - 273)] \quad (18)$$

In Eq. 18,  $k_{\text{DMS},0\text{gpg}}$  and  $k_{\text{DMS},20\text{gpg}}$  represents the kinetic constant when the hardness level is 0 and 20 gpg, respectively, and  $H$  (gpg) is the hardness of the wash liquor. The kinetic dissolution constant ( $k_i'$ ) of each FWA has been fitted using experimental data obtained by spectrophotometry and gPROMS 4.2.0 software.

### Adsorption Isotherm

It has been experimentally observed that the adsorption isotherm of FWAs is not only dependent on temperature but also on the hardness level of the solution. To consider both effects, the isotherm coefficient is expressed as described by Eq. 19 being  $a_i$ - $f_i$  parameters which have been fitted for each species  $i$  using the statistical software JMP 12

$$c_{eq,i} = a_i + b_i \cdot T + c_i \cdot T^2 + d_i \cdot H + e_i \cdot H^2 + f_i \cdot H \cdot T \quad (19)$$

In the absence of a more complex detergent formulation, the adsorption of both FWAs is significantly enhanced by the



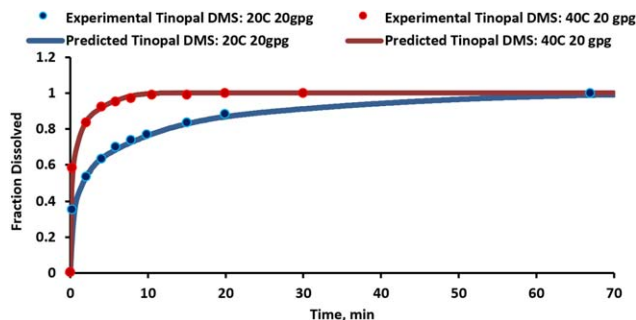


**Figure 4. Experimental and predicted dissolved fraction over time of Tinopal DMS.**

[Color figure can be viewed at [wileyonlinelibrary.com](http://wileyonlinelibrary.com)]

presence of salts ( $\text{CaCl}_2 \cdot 2\text{H}_2\text{O}$  and  $\text{MgCl}_2 \cdot 6\text{H}_2\text{O}$ ). This is in agreement with the results obtained by Yamaki et al.<sup>45</sup> who described the process as partially driven by electrostatic forces and hydrogen bonding. However, once the detergent formulation is present in the wash liquor, the effect of hardness on isotherms disappears, possibly due to the presence of all the cations within the detergent formula.

Actually, for high hardness levels in the wash liquor, the adsorption isotherm is similar to the one obtained when the detergent formulation is present. Nevertheless, when considering 0 gpg hardness the adsorption coefficient,  $c_{eq,i}$ , is approximately zero. This is believed to be due to both cotton textiles and FWAs molecules negatively charged. Thus, for those experimental conditions, it is considered that only the mass of FWAs remaining in the adsorbed water within the fabrics at the end of the experiment remains on the textiles' structure ( $\sim 2\%$ ). The effect of temperature on the adsorption isotherm is negative so that with increasing temperature the retention efficiency diminishes which is believed to be caused by increasing energy of molecules

### Dual Porosity of Fabrics

A lack of fit is observed for the deposition kinetics of FWAs on cotton fabrics when the simplified system with Fickian diffusion across a single diffusive layer is considered. The hypothesis presented to explain this disagreement between experimental and predicted data is the presence of a complex dual porosity fabric structure.<sup>24</sup> More specifically, some fibers are on the surface of the yarn while others are deeper into the yarn. Fabrics have two main porosities, inter-yarn porosity due to the spaces present in between the yarns of the textiles and intra-yarn porosity due to the spaces between the fibers forming the yarns. As a consequence, FWA molecules diffuse across different distances before they reach the fabric surface. Initially a rapid decay of the bulk concentration is observed which is thought to correspond to the adsorption of molecules on the fibers that are on the outer surface of the yarns. The rate of adsorption progressively decreases until saturation is reached leading to the diffusion to deeper areas of fabrics (intra-yarn porosity) which would promote a slower decrease of the bulk concentration due to larger diffusion distances. The deposition on the outer fibers of the yarns is fast because there is convective flow in the inter-yarn porosity so that the actual diffusive distance should be very small. The approach followed to model the process is based on assuming two different fiber surfaces differing in their surface area and diffusion distance, where molecules can diffuse and get

simultaneously adsorbed. The system can be considered analogous to an electrical system with two resistances in parallel as represented in Figure 5 where FWA flux is equivalent to electrical current, diffusive distance is equivalent to electrical resistance and concentration gradient is equivalent to the electrical potential which is equal for both diffusion distances only initially when the adsorbed concentration is zero.

The equations previously described still apply, although two different diffusive distances on different surface areas are now considered. Due to the fabric to wash liquor ratio considered in the present study, the convective transport of molecules is much faster than the diffusive process. This assumption is based on experimental results where no differences in the bulk concentration profile of FWAs were observed when different impeller speeds above 100 rpm were used. This implies that the transport in the convective region is not the limiting step for the system and conditions considered and therefore can be neglected. Under realistic washing conditions this might not be the case as the fabric to wash liquor ratio can be significantly higher (typically  $\sim 0.05$  kg:kg to 0.25 kg:kg) and the convective flow through the fabrics can be of the same order of magnitude as the diffusive flow. The mass balance for two different diffusive layers can be described by Eqs. 3 and 20

$$V_{\text{conv}} \frac{dc_{\text{conv},i,t}}{dt} = Q_F \cdot c_{\text{solution},i,t} - Q_F \cdot c_{\text{conv},i,t} - S_{A_1} \cdot D_i(T) \cdot \left. \frac{\partial c_{i,1}(x,t)}{\partial x} \right|_{x=0} - S_{A_2} \cdot D_i(T) \cdot \left. \frac{\partial c_{i,2}(x,t)}{\partial x} \right|_{x=0} \quad (20)$$

where  $L_1$ ,  $L_2$  and  $S_{A_1}$ ,  $S_{A_2}$  refers to the diffusive distance and apparent surface area of the outer and inner fabrics' surface, respectively, and  $c_{i,1}(x,t)$  and  $c_{i,2}(x,t)$  are the concentration of species  $i$  at time  $t$  and position  $x$  in the first and second diffusive layers, respectively. The mass balance to the bulk when considering instantaneous convective replenishment can be expressed as described by Eq. 21

$$V_{\text{bulk}} \frac{dc_{\text{solution},i}}{dt} = -S_{A_1} \cdot D_i(T) \cdot \left. \frac{\partial c_{i,1}(x,t)}{\partial x} \right|_{x=0} - S_{A_2} \cdot D_i(T) \cdot \left. \frac{\partial c_{i,2}(x,t)}{\partial x} \right|_{x=0} + \frac{dM_i}{dt} \quad (21)$$

The total surface area available for FWAs adsorption is still experimentally calculated considering the apparent surface area of textiles via Eq. 5 (see Table 1). Since the model considers two different surfaces where FWAs molecules can diffuse and adsorb, they can be expressed as a function of the total surface area available as described by Eq. 22

$$S_{A_{\text{specific}}} = S_{A_{\text{specific } 1}} + S_{A_{\text{specific } 2}} \\ S_{A_{\text{specific Ratio}}} = S_{A_{\text{specific } 1}} / S_{A_{\text{specific } 2}} \quad (22)$$

where  $S_{A_{\text{specific } 1}}$  and  $S_{A_{\text{specific } 2}}$  is the specific surface area of the outer and inner area of the fabrics, respectively.

The total volume of the wash liquor is given by Eq. 23

$$V_{\text{total}} = V_{\text{bulk}} + V_{\text{stagnant}}; V_{\text{stagnant}} = V_{\text{yarns}} + V_{\text{fibers}} \\ V_{\text{yarns}} = S_{A_{\text{specific } 1}} \cdot M_F \cdot L_1 \\ V_{\text{fibers}} = S_{A_{\text{specific } 2}} \cdot M_F \cdot L_2 \quad (23)$$

Unknown variables of the system are the specific surface area of textiles corresponding to the outer and inner fabrics'



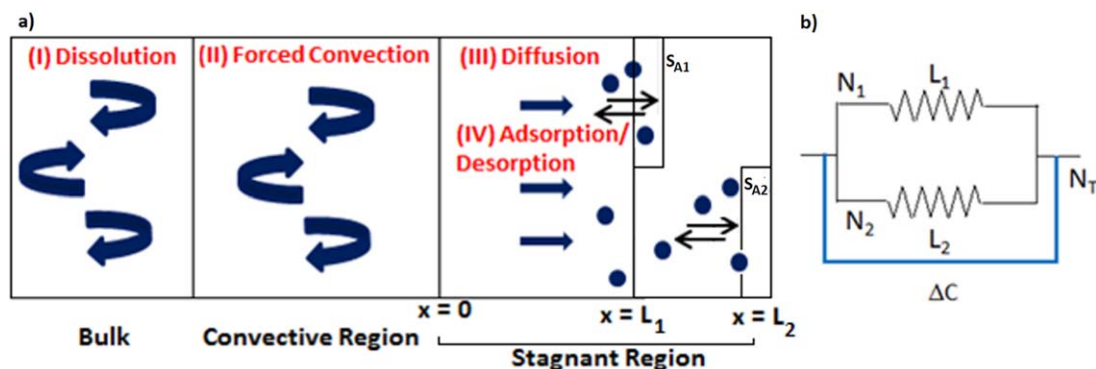


**Figure 5. (a) Schematic representation of the system considered; (b) comparison to an electrical system with two resistances in parallel.**

[Color figure can be viewed at [wileyonlinelibrary.com](http://wileyonlinelibrary.com)]

surface, the extension of the diffusive distance of the stagnant region corresponding to each of the surfaces and the diffusion coefficient of each FWA. Fitting of parameters was conducted using gPROMS 4.2.0 software.

The diffusion coefficient of each FWA was fitted considering the proposed mathematical model with a single diffusion distance to the fabric surface. For that purpose, experiments were conducted following the procedure described previously but with a stirring speed of 20 rpm. This speed corresponded to the minimum agitation required to have mixing in the system without promoting a reduction on the thickness of the stagnant layer of the fabrics due to the mechanical action. The extent of the diffusive layer, under these conditions, was assumed to be half the yarn diameter of the cotton fabrics which was experimentally measured by SEM (see Table 1). The fitted diffusion coefficient at 293 K is  $2.5 \times 10^{-10}$  and  $5.75 \times 10^{-10} \text{ m}^2/\text{s}$  for Tinopal DMS and Tinopal CBS, respectively. It can be observed that Tinopal CBS presents a higher diffusion coefficient. This can be attributed to a lower molecular weight compared to Tinopal DMS. The fitted diffusion coefficients are of similar order compared to the estimations that would be obtained using the Wilke and Chang expression.<sup>46</sup> Once the diffusivities of both FWAs are estimated, fitting of the external and internal specific surface area of the fabrics ( $S_{A\text{specific}1}$ ,  $S_{A\text{specific}2}$ ) and length of each of the diffusive layers of the stagnant region corresponding to each of the surfaces ( $L_1$ ,  $L_2$ ) is conducted using the modified proposed mathematical model obtaining the following values:  $L_1 = 3.5\text{E-}6 \text{ m}$ ,  $L_2 = 1.62\text{E-}4 \text{ m}$ ,  $S_{A\text{specific}1} = 0.6285 \text{ m}^2/\text{kg}$  and  $S_{A\text{specific}2} = 11.7515 \text{ m}^2/\text{kg}$ . It can be observed that the distance to the outer surface of the fabrics ( $L_1$ ) is very short as it is easily accessible by molecules. However deeper areas of the fabrics which are not directly exposed to the wash liquor present a higher diffusion distance which is similar to the measured yarn diameter. Interestingly, this fabric structure has a maximum thickness of two times the yarn diameter because of the interlacing of the yarns. It is important to bear in mind that the fitted parameters  $L_1$  and  $L_2$  are model effective diffusion distances for the system considered where the complex 3-D geometry of the cotton textiles has been simplified to a 1-D Cartesian system. Figure 6 represents both the experimental and predicted profiles of bulk concentration over time for Tinopal DMS modeled when considering a single and a double diffusive layer. One can see how the latter predicts the experimental behavior more accurately, that is, the maximum error of the predictions is  $\sim 1.5\%$  vs. up to  $\sim 37\%$  (at long times)

obtained when considering a single diffusive distance. Similar results are obtained when considering Tinopal CBS. The initial increase in bulk concentration is due to the dissolution of FWAs. At time  $t = 900 \text{ s}$  fabrics are introduced in the tergotometer causing a decay in the bulk concentration due to the FWAs deposition on the fabrics' structure until equilibrium is reached. It is important to notice that in the case of Tinopal DMS, full dissolution is not achieved when the fabrics are added to the wash liquor, which is also accounted by the model.

#### Model evaluation

Evaluation of the proposed model for the adsorption of FWAs on flat cotton fabrics is carried out by comparing experimental adsorbed concentration of FWAs on textiles across all conditions and the predicted adsorbed concentration by the model obtaining an  $R^2$  of 0.920 and 0.979 for systems containing Tinopal DMS and Tinopal CBS, respectively.

#### Multicycle performance

To be able to predict multicycle performance, an understanding of the degradation of FWAs between washes due to UV light exposure is required. A decrease on the  $db_{i,t}^*$  value measured under D65 standard illuminant conditions after the exposure of textiles to sunlight has been observed. It is believed to be due to the oxidative degradation of FWAs leading to loss of fluorescence. The decrease on  $db_{i,t}^*$  was observed to be approximately constant after each cycle and more pronounced for those textiles containing Tinopal DMS. However,  $db_{i,t}^*$  values of textiles under D65 with nil UV component also decrease after the exposure indicating that the base white of fabrics is improving with the action of sunlight; further experimental work is required to better understand the transformations taking place leading to this behavior.

#### Impact of dissolution kinetics on performance

Performance of FWAs may be significantly impacted by the dissolution kinetics as only dissolved mass is depositing on the fabrics' structure. To study the impact of dissolution on Tinopal DMS performance, several experiments were carried out following the procedure previously described but in this case, after the addition of 0.8-L deionized water at 293 K to the tergotometer, salts corresponding to 20 gpg hardness level, the detergent formulation (5000 ppm) and Tinopal DMS (35.1 ppm) were simultaneously added to the tergotometer. Unbrightened cotton fabrics were immediately added

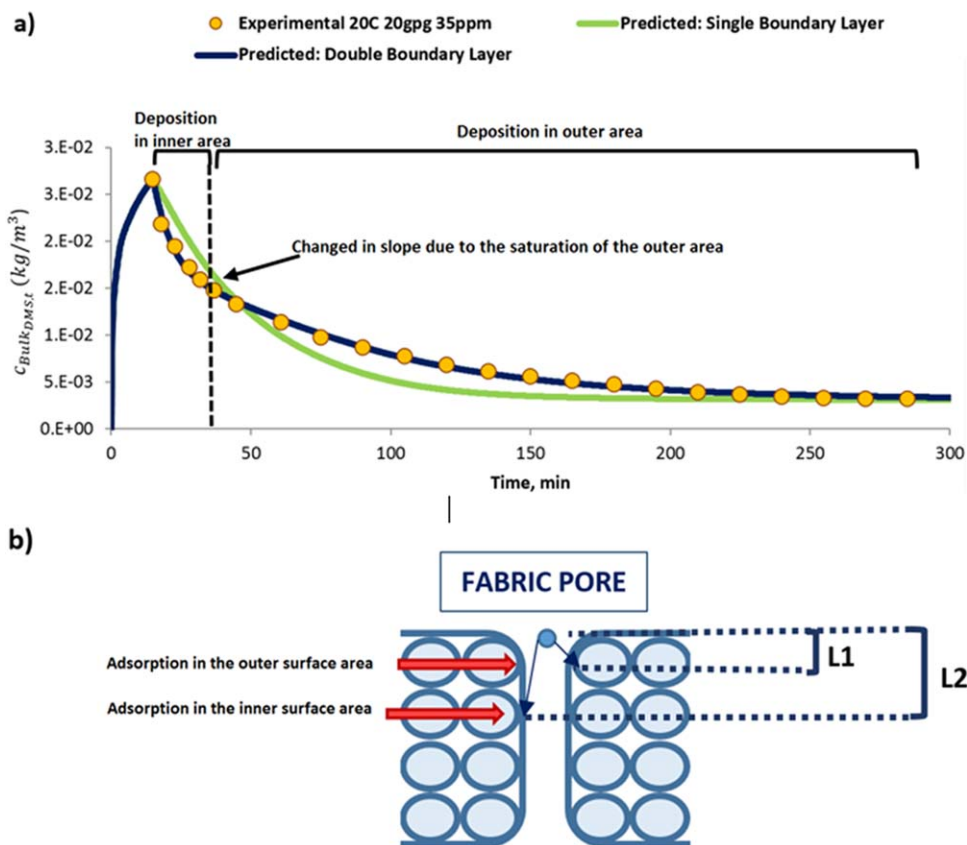


**Figure 6. (a) Experimental and predicted profile of Tinopal DMS bulk concentration for 20C, 20 gpg, and 35 ppm initial concentration.**

[Color figure can be viewed at [wileyonlinelibrary.com](http://wileyonlinelibrary.com)]

afterward without leaving any time for the dissolution of any of the species. The textiles were left in the solution for different contact times (5, 10, or 20 min) and the stirring speed was maintained constant during the entire experiment at 100 rpm. Finally, the cotton fabrics were removed from the wash liquor and dried overnight at room temperature prior to conduct the measurement of  $L^*a^*b^*$  values. Table 2 summarizes the experimental and predicted  $db_{n,i,t}^*$  values for experiments conducted with and without predissolution for Tinopal DMS. As it can be observed, there are significant differences for short contact times, whereas for 20 min where ~80% of Tinopal DMS has been already dissolved for these specific experimental conditions (Figure 4) there is no measurable difference on the resulting  $db_{n,i,t}^*$  of the textiles.

#### Fabric to wash liquor ratio

For a fixed fabric to wash liquor ratio, the adsorbed concentration of FWAs on textiles increases with increasing initial concentration of active in solution. However, deposition time

to reach 95% of the equilibrium concentration does not vary. Although there is more mass of chemistry to get adsorbed, the concentration gradient also increases, and therefore promotes a higher diffusive flux toward the fabric surface as described by Fick's law. However, the time to reach 95% of the equilibrium concentration as well as the actual equilibrium concentration increase with decreasing fabric to wash liquor ratio for a fixed FWAs concentration in solution since there is more mass of active per surface area of textiles to be adsorbed. Therefore, depending on the type of washing machine, where the fabric to wash liquor ratio can vary significantly (typically ~0.05 kg/kg to 0.25 kg/kg), washing times play a key role on the final FWA adsorbed on fabrics and thus, on the resulting whiteness of textiles requiring almost twice the time for actives in the lower fabric to wash liquor ratio machine to reach equilibrium. Figure 7 represents the bulk concentration of Tinopal CBS over time for different fabric to wash liquor ratios maintaining the chemistry to wash liquor ratio constant in all cases. It can be observed how the bulk concentration is decreasing more rapidly at high fabric to wash liquor ratios as previously mentioned. It is important to bear in mind that in the case of a washing machine with a high fabric to wash liquor, the convective flow through fabrics (not considered in Figure 7) would limit the deposition process.

#### Impact of fabric structure on brightener performance

Different cotton fabric types (i.e., knitted cotton, flat cotton, polycotton, and terry towel) have different weaving structures which imply different fabric thicknesses resulting in lower apparent surface areas for those fabrics with higher thickness

**Table 2. Experimental  $db_{n,DMS,t}^*$  of Textiles with and Without Predissolution of Tinopal DMS Prior to the Addition of Textiles**

Time (min)	No predissolution		Predissolution	
	Experimental $db_{n,DMS}^*$	Predicted $db_{n,DMS}^*$	Experimental $db_{n,DMS}^*$	Predicted $db_{n,DMS}^*$
5	0.621	0.623	0.782	0.720
10	0.771	0.776	0.838	0.833
20	0.887	0.852	0.878	0.872

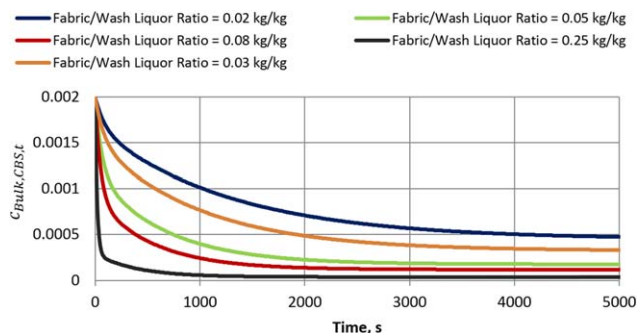


**Figure 7. Effect of fabric to wash liquor ratio on the deposition kinetics and equilibrium concentration for a constant initial FWA concentration.**

[Color figure can be viewed at wileyonlinelibrary.com]

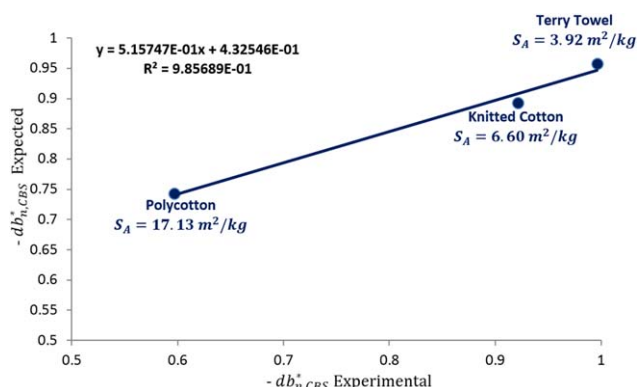


**Figure 8. Expected vs. experimental  $db_n^*$  of Tinopal DMS for different cotton fabric structures.**

[Color figure can be viewed at wileyonlinelibrary.com]

(more mass per area). This could have an impact on the performance of FWAs adsorbing on its structure.

Figure 8 shows the experimental benefit observed when experiments are conducted using textiles with different structure (terry cotton, polycotton and knitted cotton) vs. the predicted benefit that would be obtained by the proposed mathematical model taking into account the apparent surface area of each textile type. The experiments were conducted

following the methodology previously described at 293 K, 0 gpg hardness, 0.01875 kg/kg fabric to wash liquor ratio, and 7.8 ppm of initial concentration in solution of Tinopal CBS.

The hypothesis presented is that similar concentration of FWAs is adsorbing per unit mass of textile or per fiber due to similar fiber diameter of all the textiles (see Table 1). Thus, higher adsorbed concentration of FWAs per apparent surface area is expected for thicker fabrics (in agreement with experimental results shown in Figure 8). As FWAs deposit on fabrics, there are two limiting cases between which all possible scenarios fall: (i) FWAs are mainly adsorbing on the external surface of the yarns which could lead to quenching of reflectance (lower  $db_{i,t}^*$  of fabrics than expected for the FWA adsorbed concentration, Figure 9a) due to having several layers of FWAs, (ii) FWAs are also diffusing to deeper areas of yarns because of the external surface is getting saturated. In this case, FWAs in deeper areas could also contribute less to the final  $db_{i,t}^*$  than those FWA molecules adsorbing in more superficial layers (Figure 9b). Circles in Figure 9 represent the fibers of the cotton textiles while the small dots represent the FWA adsorbed.

It can be observed that a slope of  $\sim 1$  is obtained in Figure 8. This suggests that the  $db_{i,t}^*$ -adsorbed concentration relationship previously modeled for flat cotton fabrics (Eq. 14) still applies and therefore there is no significant quenching of reflectance due to the differences in the thickness of the fabrics. Thus, by modeling one fabric structure, whiteness performance can be predicted across any fabric structure as long as the specific surface area ( $m^2/kg$ ) is known.

## Conclusions

In this study, we investigated the adsorption of two widely used stilbene derivative FWAs on unbrightened and unbleached flat cotton fabrics as a function of temperature of the wash liquor, fabric to wash liquor ratio, initial concentration of FWAs in solution, hardness, and concentration of a commercial detergent with nil FWAs content. The adsorption isotherm of the FWAs is enhanced by the presence of salts in the wash liquor which may be due to electrostatic forces partially driving the process. Temperature has a negative effect on the adsorption isotherm of both FWAs which could be caused by an increase on the energy of molecules with increasing temperature leading to lower deposition efficiency. Deposition time to reach 95% of equilibrium as well as equilibrium concentration increase with decreasing fabric to wash liquor ratio for a fixed FWA

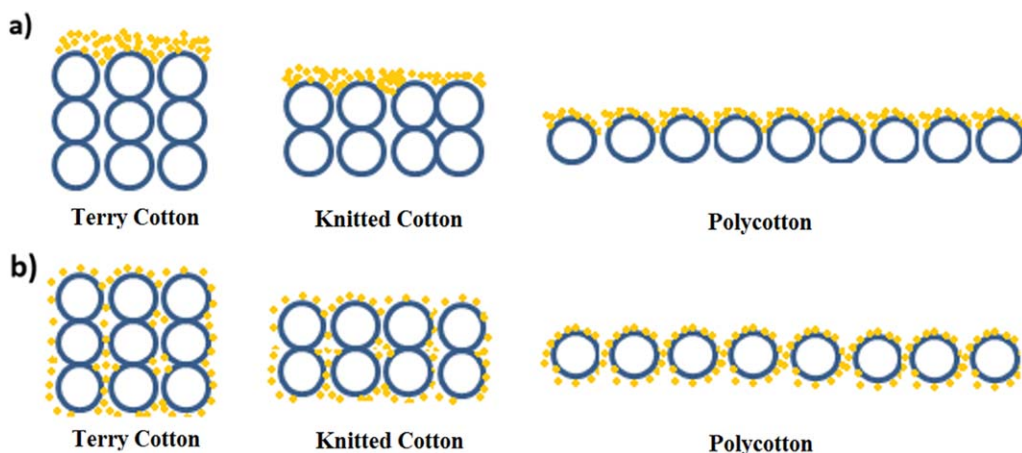


**Figure 9. Schematic representation of FWAs adsorption on different types of cotton fabrics.**

[Color figure can be viewed at wileyonlinelibrary.com]



concentration since there is more mass of active per surface area to be adsorbed and the system equilibrates at a higher adsorbed concentration in the isotherm curve. Therefore, depending on the type of washing machine where the fabric to wash liquor ratio can vary significantly (typically  $\sim 0.05$  kg/kg to  $0.25$  kg/kg), the time of the main wash cycle plays a key role on the final amount of FWA adsorbed on the fabrics and therefore on the resulting whiteness of the textiles requiring almost twice the time for actives in the lower fabric to wash liquor ratio machine to reach equilibrium.

Based on experimental data, a mechanistic model has been developed to describe the dissolution process of FWAs, convective mass transport into the fabrics, diffusion to the fabrics surface in the stagnant layer of yarns and adsorption on the fabrics structure. Dissolution of FWAs has a great impact on whiteness performance so that for short and cold washing cycles where dissolution is slower, whiteness performance decreases significantly. These results are in agreement with predictions obtained by the mathematical model. Dual porosity (inter-yarn and intra-yarn porosity) of the fabrics is considered in the model by allowing two different regions in the fabrics where FWAs molecules can diffuse and adsorb. Each region represents the outer and inner surfaces of fabrics, respectively, which have a different surface area and diffusion distance. Good agreement between experimental data of FWAs depositing on cotton fabrics and predicted data by the proposed model is observed for the range of variables considered. The approach followed to model the deposition of FWAs on textiles as well as the key learnings can be reapplied to any other depositing molecular active present in the washing cycle.

## Acknowledgments

We would like to thank the Engineering and Physical Sciences Research Council (EPSRC), (UK) and Procter and Gamble, (UK) for funding this project.

## Literature Cited

- Kramer JB. Fluorescent whitening agents. In: Hutzinger O, editor. *The Handbook of Environmental Chemistry: Volume 3, Part F. Anthropogenic Compounds*. Berlin: Springer, 1992:351–366.
- Lim SH, Lee JJ, Hinks D, Hauser P. Bleaching of cotton with activated peroxide systems. *Coloration Technol*. 2005;121(2):89–95.
- Pereira L, Bastos C, Tzanov T, Cavaco-Paulo A, Guebitz GM. Environmentally friendly bleaching of cotton using laccases. *Environ Chem Lett*. 2005;3(2):66–69.
- Rounds MAJ, Purchase ME, Smith BF. Fatty soil retention and the influence of particulate and fatty soils on yellowing of an unfinished dacron/cotton blend fabric. *Textile Res J*. 1973;43(9):517–523.
- Chi YS, Obendorf SK. Aging of oily soils on textiles materials: a literature review. *J Surfact Deterg*. 1998;1(3):407–418.
- Chi YS, Obendorf SK. Aging of oily soils on textiles. Chemical changes upon oxidation and interaction with textile fibres. *J Surfact Deterg*. 1998;1(3):371–380.
- Chi YS, Obendorf SK. Effect of fibre substrates on appearance and removal of aged oily soils. *J Surfact Deterg*. 2001;4(1):35–41.
- Iamazaki EI, Atvars T. Role of surfactants in the sorption of the whitening agent tinopal CBS onto viscose fibres: a fluorescence spectroscopy study. *Langmuir*. 2006;22(24):9866–9873.
- Siegrist AE, Eckhardt C, Kaschig J, Schmidt E. Optical brighteners. In: Elvers B, editor. *Ullmann's Encyclopedia of Industrial Chemistry* (Vol 25). Weinheim, Germany: John Wiley & Sons, 2003:427–449.
- Waldhoff H, Spilker R. *Handbook of Detergents Part C: Analysis*. New York, NY: Marcel Dekker, 2004.
- Deo HT, Desai BK. Dyeing of cotton and jute with tea as a natural dye. *Coloration Technol*. 1999;115(7–8):224–227.
- Kramer JB, Canonica S, Hoigné J, Kaschig J. Degradation of fluorescent whitening agents in sunlit natural waters. *Environ Sci Technol*. 1996;30(7):2227–2234.
- Dyer JM, Cornellison CD, Bringans SD, Maurdev G, Millington K. The photoyellowing of stilbene-derived fluorescent whitening agents—mass spectrometric characterization of yellow photoproducts. *Photochem Photobiol*. 2008;84:145–153.
- Assaad A, Pontvianne S, Pons MN. Photodegradation—Based detection of fluorescent whitening agents in a mountain river. *Chemosphere*. 2014;100:27–33.
- Kaschig J, Schaumann M, Schultz B. The photochemistry of fluorescent whitening agents: impact of lightfastness. In: Cahn A, editor. *Proceedings of the 4<sup>th</sup> World Conference on Detergents: Strategies for the 21<sup>st</sup> Century*. Montreux, Switzerland: AOCS Press, 1999: 323–325.
- Mac Namara C, Gabriele A, Amador C, Bakalis S. Dynamics of textiles motion in a front-loading domestic washing machine. *Chem Eng Sci*. 2012;75:14–27.
- Choi JW, Choi NC, Lee SJ, Kim DJ. Novel three-stage kinetic model for aqueous benzene adsorption on activated carbon. *J Colloid Interface Sci*. 2007;314(2):367–372.
- Matsui H, Kobayashi M, Koji K. Washing of fabrics part I: washing of cotton fabrics and its theoretical analysis. *J Textile Eng*. 1978;24: 41–49.
- Gooijer H, Warmoeskerken MMCG, Wassink JG. Flow resistance of textile materials, part I: monofilament fabrics. *Textile Res J*. 2003; 73(5):437–443.
- Gooijer H, Warmoeskerken MMCG, Wassink JG. Flow resistance of textile materials, part II: multifilament fabrics. *Textile Res J*. 2003; 73(6):480–484.
- Van den Brekel L. *Hydrodynamics and mass transfer in domestic type fabric washing machines* [PhD thesis]. Delft, the Netherlands: Delft University of Technology, 1987.
- Moholkar VS, Warmoeskerken MMCG. Investigations in mass transfer enhancement in textiles with ultrasound. *Chem Eng Sci*. 2004;59(2): 299–311.
- Ganguli KL, Eendenburg JV. Mass transfer in a laboratory washing machine. *Textile Res J*. 1980;50(7):428–432.
- Warmoeskerken MMCG, Van der Vlist P, Moholkar V, Nierstrasz V. Laundry process intensification by ultrasound. *Colloids Surf A: Physicochem Eng Aspects*. 2002;210(2–3):277–285.
- Yoon SH, Chai XS. Adsorption for polymeric additives in paper-making aqueous fibrous media by UV spectroscopic analysis. *Bull Korean Chem Soc*. 2006; 27:1–10.
- Chai XS, Yoon SH. UV spectroscopic monitoring method for real time wet end control of polymeric adsorption in aqueous fibrous suspensions. *J Ind Eng Chem*. 2007;13:244–249.
- XianNan H, YanGui H, XinSheng C, Wei W. Study of adsorption kinetics for fluorescent whitening agent on fibre surfaces. *Sci China Ser B: Chem*. 2008;51(5):473–478.
- Iamazaki EI, Atvars T. Sorption of fluorescent whitening Agents (Tinopal CBS) onto modified cellulose fibers in the presence of surfactants and salt. *Langmuir*. 2007;23(26):12886–12892.
- De Boer LM. Water hardness and domestic use of detergents. *Am Water Works Assoc*. 1961;53:809–822.
- Goodwin J. *Colloids and Interfaces with Surfactant and Polymers—An Introduction*, 2nd ed. Chichester, UK: John Wiley & Sons, 2004.
- Elimelech M, Gregory J, Ha X, Williams R. *Particle Deposition and Aggregation, Measurement, Modelling and Simulation*. Butterworth-Heinemann Ltd., 1995.
- Stana KK, Pohar C, Ribitsch V. Adsorption of whitening agents on cellulose fibres—monitored by streaming potential measurements calorimetry and fluorescence. *Colloid Polym Sci*. 1995;273(12): 1174–1178.
- McDonald R. *Colour Physics for Industry*, 2nd ed. Bradford, UK: Society of Dyers and Colourists, 1997.
- Schanda J. *Colorimetry: Understanding the CIE System*. Hoboken, NY: John Wiley & Sons, 2007.
- Homann JP. *Digital Color Management. Principles and Strategies for the Standardized Print Production*. Berlin, Germany: Springer, 2009.
- Lim YK, Lee YK. Fluorescent emission of varied shaded of resin composites. *Dental Mater*. 2007;23(10):1262–1268.
- Koganti V, Carroll F, Ferraina R, Falk R, Waghmare Y, Berry M, Liu Y, Norris K, Leasure R, Gaudio J. Application of modelling to scale-up dissolution in pharmaceutical manufacturing. *AAPS Pharm Sci Tech*. 2010;11(4):1541–1548.
- Noyes AA, Whitney WR. The rate of solution of solid substances in their own solutions. *J Am Chem Soc*. 1897;19(12):930–934.

39. Cao H, Amador C, Jia X, Li Y, Ding Y. A modelling framework for bulk particles dissolving in turbulent regime. *Chem Eng Res Design*. 2016;114:108–118.
40. Crank J. *The Mathematics of Diffusion*, 2nd ed. Oxford, UK: Oxford University Press, 1979.
41. Kholodenko LA, Douglas JF. Generalized Stokes-Einstein equation for spherical particle suspensions. *Phys Rev E*. 1995;51(2):1081–1090.
42. Perry RH, Green DW, Maloney JO. *Perry's Chemical Engineers' Handbook*, 7th ed. New York, NY: Mc Graw Hill, 1997.
43. Foo KUY, Hameed BH. Insights into the modelling of adsorption isotherm systems. *Chem Eng J*. 2010;156(1):2–10.
44. Raaijmakers JGW. Statistical analysis of the Michaelis Menten equation. *Biometrics*. 1987;43(4):793–803.
45. Yamaki SB, Barros DS, Garcia CM, Socoloski P, Oliveira ON, Atvars TDZ. Spectroscopic studies of the intermolecular interactions of congo red and tinopal CBS with modified cellulose fibres. *Langmuir*. 2005;21(12):5414–5420.
46. Coulson JM, Richardson JF, Backhurst JR, Harker JH. *Coulson & Richardson's Chemical Engineering*, 6th ed. (Vol. 1). Oxford, UK: Butterworth–Heinemann, 1999.

*Manuscript received Mar. 18, 2017, and revision received July 7, 2017.*